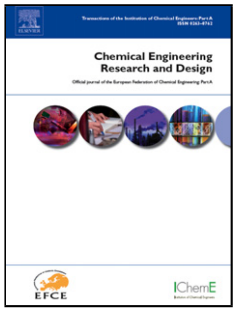

Title: Formulation optimization of reverse microemulsions using design of experiments for nanoparticle synthesis

Authors: Ehsan Nourafkan, Hui Gao, Zhongliang Hu, Dongsheng Wen

PII: S0263-8762(17)30398-2
DOI: http://dx.doi.org/doi:10.1016/j.cherd.2017.07.023
Reference: CHERD 2764

To appear in:

Received date: 30-3-2016
Revised date: 28-4-2017
Accepted date: 14-7-2017

Please cite this article as: Nourafkan, Ehsan, Gao, Hui, Hu, Zhongliang, Wen, Dongsheng, Formulation optimization of reverse microemulsions using design of experiments for nanoparticle synthesis.Chemical Engineering Research and Design http://dx.doi.org/10.1016/j.cherd.2017.07.023

Formulation optimization of reverse microemulsions using design of experiments for nanoparticle synthesis

Ehsan Nourafkan[1], Hui Gao[1], Zhongliang Hu[1] and Dongsheng Wen[2,1*]

[1]School of Chemical and Process Engineering, University of Leeds, Leeds, LS2 9JT, U.K.

[2]School of Aeronautic Science and Engineering, Beihang University, 100191, P.R.China

*Corresponding author. Tel.: +44 (0)113 3431299
d.wen@buaa.ac.uk (D. Wen)

Research highlight

- Optimized formation of reverse microemulsion (RM) for nanoparticle synthesis was studied
- The RM was obtained by using the Box-Behnken(3^3) experimental design method
- The effect of pH, cosurfantant amount and HLB on RM were studied
- RM with average size of 42 nm and polydispersity index of 0.41 was achieved
- Spherical Fe_2O_3 nanoparticles with 2 nm size were obtained using optimized RM.

Abstract

The present work investigates the development of water/mixed nonionic surfactant/co-surfactant/cyclohexane reverse microemulsions (RM)suitable for nanoparticles synthesis. The mixture of Span 80 (oil soluble) and Tween 80 (water soluble) was selected as the surfactants. Optimum formulation of RM was obtained by using the Box-Behnken (3^3) experimental design method to evaluate the effect of three independent process variables, i.e., pH, Span 80 wt% in surfactant mixture, and propyl alcohol wt% in mixture of cyclohexane and propyl alcohol, on the preferred responses: average droplet size (ADS) and polydispersity index (PDI) of droplets. The model was validated experimentally based on an ANOVA table, and was optimized to reach the optimum formulation to yield the ADS and PDI for RMs.The determination coefficient (R^2)

values of 0.991for ADS and 0.975 for PDI show that Box-Behnken design is a useful platform for the optimization of RMs formulation. Finally, iron oxide nanoparticles were synthesized under the optimum RM conditions and the uniform nanoparticle distribution with an average particle size of 2.1±0.49 nanometer and a polydispersity of 0.06±0.011 were obtained.

Abbreviation and Nomenclature

ADS	Average droplet size [nm]
b_i	First-order (linear) main effect
b_{ii}	Quadratic (squared) effect
b_{ij}	Interaction effect
C.V.	Coefficient of variation
df	Degree of freedom
DOE	Design of experiment
IFT	Interfacial tension
k	Factor number
HLB	Hydrophilic-lipophilic balance
n	Number of experiment
PDI	poly dispersity index
r	Replicate number of the central point
R^2	Determination coefficient
RM	Reverse microemulsion
SS	Computed sum of squares
TPC	Total percentage contributions
Y	Process response
Y_p	Predicted values by quadratic equation
Y_o	Experimental value
$\bar{Y}_o$	Average of experimental values
α	Level of significance
Φ	Objective function

ε Error

Keywords: Reverse microemulsions, Box-Behnken experimental design, Iron oxide nanoparticles, Span80/Tween80,Cosurfactant.

1.Introduction

Droplet microemulsion or swollen micelle system are colloidal dispersions, i.e., a suspension of small oil droplets (radius<100 nm) in an aqueous medium that stabilized by surfactants/co-surfactant monolayer. Microemulsion as an isotropic one phase solution is optically clear and thermodynamically stable [1]. The term of microemulsion was firstly used by Schulman and coworkers [2] to describe a homogenous opaque solution in a water- benzene and Potassium oleate system. After the addition of a short chain alcohol as a co-surfactant, the solution was found to become clear, having a droplet size distribution in the range of 600 ~ 8000 nm, hence microemulsions was named and used subsequently [3, 4]. After the discovery, microemulsions have found a wide range of applications in oil recovery [5], food [6], cosmetic [7] and synthesis of nanoparticles [8]. Similarly, water swollen micelle dispersed in a continuous oil phase is called reverse microemulsions (RM) where the polar head groups of surfactant or co-surfactant molecules are attracted to the aqueous phase droplets while the hydrocarbon chain (non-polar part) is attracted by oil phase.

In recent years, the synthesis of inorganic nanoparticles using the RM method has received considerable interests [4].A wide range of metallic, metallic oxide and ferrite nanoparticles have been produced using this method [9-11]. Nanometer sized and monodispersed water droplets in RM make it a versatile method to fabricate nanoparticles with controlled morphology [12, 13], surface area [14, 15] and uniform size distribution [16, 17]. In this method, two different RMs containing precursors of a desired reaction are mixed together, where the surfactant-covered water droplets act as nano-reactors. The droplets collide each other driven by the Brownian motion or under an external field causes the fusion of droplets. Subsequently chemical reaction occurs inside the droplet, including the formation of primary nuclei, followed by growth

mechanism and finally stabilization of nanoparticles, as illustrated schematically in Fig. 1. Among various influencing factors, the average droplet size (ADS) and polydispersity index (PDI) of RM have the greatest influence on size and uniformity on produced nanoparticles [18].

A number of RM parameters, such as surfactant/oil ratio, water/oil ratio or type of oil phase on ADS and PDI,have been investigated in the past [19, 20].For instance, it has been found that increasing water/oil or water/surfactant ratio would produce large ADS[21].However, the influence ofa few other parameterssuch as cosurfactant amount, hydrophilic-lipophilic balance (HLB) and pHfor different RMs requires further study, as briefly reviewed below.

For any emulsion system, the choice of a right surfactant is critical. It has been shown that using a single surfactant alone is usually not sufficient to produce stable RMs[22]. The structure and HLB value of surfactant have been found to be the key factors for the formation of RM with a minimal ADS and PDI[23, 24]. To obtain an optimum HLB value, appropriate mixing of surfactants with different HLB values is aneffective way, as shown in Eq. (1), for a binary surfactant mixture:

$$HLB_{mix} = x_1 HLB_1 + x_2 HLB_2 \quad (1)$$

where x_1 and x_2 are the mass fraction of the two surfactants with HLB_1 and HLB_2, respectively, and HLB_{mix} is the HLB value of the mixture. Depending on the system used, different HLB values have been reported in literature. Williams [25]suggested that a good HLB value for RM formation was between 3 and 6. Noor El-Din et al.[26]showed that at HLB=10, a minimum droplet size of 49.55 nm with a smallest Ostwald ripening can be obtained for amixed sorbitanmonooleate and polyoxyethylene (20) sorbitanmonooleate surfactants on water-in-diesel RMs.

Using co-surfactants (e.g. short or medium-chain alcohols, polymers, amines) is an effective way to reduce the surface interfacial tension (IFT) of dispersed water phase in a RM.A low IFT would compensatea large increase in the dispersion entropy, forminga stable microemulsion [27].Co-surfactant molecules would form complex structures at the interfacial region of water droplets and the continuous oil phase, which would change the solubility of surfactant molecules and reduce the repulsions between the hydrophilic head groups.It has shown that the phase behavior of microemulsions in the presence of co-surfactant is of high importance in determining

their functions [28-31].In this aspect, Mathew and Juang [32]conducted a review on the role of alcohols on the formation of RMs. Azeem et al. [33]proposed ascreening criterionfor proper selection of oil, surfactant, and cosurfactants to formproper nanoemulsions. By combining Tween surfactant with six different types of cosurfactants of ethanol, isopropyl alcohol, n-butanol, PEG 400, Carbitol, and propylene glycol, it was found that the parameters range of the existence of nanoemulsion was extended if the chain length of alcohol was increased and the number of hydroxyl groups was decreased.Yang et al.[34] showed that the presence of a cosurfactant favored the modulation of the strength of surfactant film and the exchange dynamics of micelles, and a goodcrystallinity of formed nanoparticles could be achieved.

Another important factor in RM formation is the pH value,which has considerable effect on the characteristics of final produced nanoparticles [9, 35].DifferentpH values affect theionization of head groups of surface active components and the formation of different droplet sizes[36].The reducingagent inside droplets (e.g. sodium hydroxide, hydrazine) would produce an alkali medium insideRM and the high concentration of alkali agent in water phase wouldddeteriorate the structure of RM.

However, the majority of works on the effect of pH on reverse emulsion stability was related to the dispersion of water droplets in crude oil [37, 38]. In crude oil, the heavy components such as asphaltenes contain both acidic and basic components, and any change in pH of the water phase would affect the stability of reverse emulsion. In general, introducing inorganic acids oralkali would influence the ionization in the interfacial covering layer of emulsion droplets and modify their stabilities. This effect depends on the nature of the covering layer, but in general, alow pH would produce more stable water-in-oil emulsions whereas a high pH value would increase the stability of oil-in-water emulsions[39, 40]. A recent study by Daaou and Bendedouch [41]also showed the least stable reverse emulsion was in weakly acid environment caused by the adsorption of native surface active compounds in the crude at the oil/water interface.

The complicated effects of different parameters on RM behavior demand more experimental analysis to find the optimum conditions. The traditional optimization process involving the trial-and-error methodology is very time consuming and low efficient because of the inter-dependency of various parameters. An appropriate alternative way is to use the design of

experiment (DoE) method. Many studies have shown that properly conducted, DoE can provide high efficient optimization for forming microemulsions [21, 42, 43]. For example Pey et al.[21] obtained an optimized composition and preparation method for microemulsions of water/Tween20/Span20/liquid paraffin by using the DoE technique, and revealed a linear dependence of the droplet size on the oil/surfactant ratio. A smaller ADS could be obtained ata higher surfactant amount, but a quadratic dependence of droplet size with Tween20 percentage was observed based on the optimal Tween20/Span20 ratio. It shall be noted, however,that the DoE is not a physical model that describes the real behavior of the process, but provide a strategy for optimizing microemulsion conditions.

Above short review suggests that many parameters could affect the ADS and PDI of RMs, and many uncertainties still exist regarding the influence of the HLB, cosurfactant and pH values. Though DoE technique has been used to optimize oil in water microemulsions, few studies on RMs[44] has been conducted, especially considering the conflicting parameters. This work aims to develop a high potential RM for nanoparticle synthesis based on a ternary cyclohexane/nonionic surfactant mixture/water and obtain optimized parameters through the DoE method. As an example study, iron oxide nanoparticles are produced from RM droplets, and the DoE methodology is applied to evaluate the simultaneous effect of pH, HLB value and co-surfactant amount as the significant variables on the PDI and ADS of RMs. The nonionic mixture of Span 80 (oil soluble) and Tween 80 (water soluble) that makes different HLB values were chosen as the surfactants. The sorbitan derivatives (Span), polysorbate derivatives (Tween) and dioctylsulfosuccinate sodium (AOT) are common efficient surfactants for the formation of RMs [45].

2.ExperimentalProcedure

2.1.Materials

Analytical grade materials including cyclohexane, sorbitanemonooleate (Span 80, HLB=4.3), polyethylene glycol sorbitan monolaurate (Tween 80, HLB=15), gum Arabic, polyvinylpyrrolidone (PVP), poly ethylene glycol (PEG 2000), propyl alcohol, octyl alcohol, 1,2-propanediol, hydrochloric acid, sodium hydroxide, ferric chloride ($FeCl_3$), ferrous chloride ($FeCl_2$), were purchased from Sigma-Aldrichand used without further processing.

2.2.ReverseMicroemulsion Formation

The RMs were prepared by continuous dropwise addition of 1 ml de-ionized water into a8 ml cyclohexane and1 g Span80-Tween80mixture,which was previously homogenized. Different weight percentages of Span 80 in surfactant mixture comprising 0, 20, 40, 60, 80 and 100percentages were considered to evaluate the effect of HLB value. The equivalent HLB values were 15, 12.86, 10.72, 8.58, 6.44 and 4.3 for the mentioned weight percentages above. The effect of polymeric cosurfactants (PEG 2000, gum arabic and polyvinylpyrrolidone), alcohols (propyl alcohol, octyl alcohol) and diol (1,2-propanediol) was investigated on the stability of RMs.The pH of water phase was prepared by mixing adequate amounts of sodium hydroxide to get alkali pH (7-11), and acidic pH (3-7) was adjusted by chloridric acid.

2.3.Synthesis of Iron Oxide Nanoparticles

The massart co-precipitation method was considered for the production iron oxide nanoparticles according to the following reaction [46]:

$$FeCl_2 + 2\,FeCl_3 + 8NaOH \rightarrow Fe_3O_4 + 8NaCl + 4H_2O \quad (2)$$

The RMs containing $FeCl_3$(0.04 M) and $FeCl_2$(0.02 M) were produced based on the final optimum RM conditions at room temperature. Here 0.5 ml of sodium hydroxide (0.16 M) solution as the precursor for the reaction was added drop wise to RMs in a 10minutes duration. The mixture was stirred continuously for 4 hours to reach the equilibrium.

2.4. Reverse Emulsion and Nanoparticles Characterization

The ADS and PDI of droplets in RMs were measured by the dynamic light scattering technique using a Zetasizer (Malvern Zetasizer ZS). Five times of droplet size distribution measurement were conducted and were used for the estimation of standard deviation of ADS and PDI (i.e., each time is average of 10 trials with 1 second time step in between).In addition, the formation of different RMs was observed using an optical microscope (U-25ND6-Olympus) at 20× magnification for more clarity. The stability of emulsions was monitored using the Turbiscan Lab Expert. The pH value was measured by a digital pH meter (Model HI-208

Hanna). Viscosities of RMs were measured using a Physica Anton Paarrheometer, model MCR 301 (Cone plate CP75-1). Shear curves from 10-1000 s^{-1} were recorded at 22 °C.The morphology and size distribution of produced iron oxide nanoparticles were analyzed by Transmission electron microscope (FEI Tecnai TF20 TEM). High resolution TEM (FEI Titan Themis 300), which is equipped with super-X EDX system with 4-detector also was used to study the crystal lattice and elemental composition of nanoparticles.The size distributionof iron oxide nanoparticles was estimated based on the image processing of TEM photos with photoshop 7 software for at least 100 nanoparticles.

3.Response Surface Method

3.1. Box-Behnken Design Method

Response surface method(RSM) is an attractive optimization design tool inmany practical engineering applications and consists of three main steps [47].The 3^3(three-factor and three-level)Box-Behnken factorial design was chosen as the RSM method to evaluate the formulation of RMs[48].Three experimental design variables (X_1,X_2, andX_3)were selected as pH: X_1, propyl alcohol weight percentage in the mixture of cyclohexane and propyl alcohol: X_2,and Span 80wt% in surfactant mixture: X_3,which will be discussed in detail in Section 4.1.

The number of experiments (n) needed for the development of Box-Behnken matrix is defined as n=2k(k-1)+r, where k is the factor number (k=3) and r is the replicate number (r=5) of the central point.So a total of 17 experiments have been employed in this work to evaluate the effects of the three main independent variables. The statistical experimental data were analyzed by the Minitab 16 software.The interaction of independent variables and measured responses were modeled using the following quadratic mathematical model [49].

$$Y = b_0 + \sum_{i=1}^{K} b_i X_i + \sum_{i=1}^{K} b_{ii} X_i^2 + \sum_{i=1}^{K} \sum_{j>1}^{K} b_{ij} X_i X_j + \varepsilon \qquad (3)$$

where Y is the process response or output (dependent variable), k is the number of the patterns, i and j are the index numbers for pattern, b_0 is the free or offset term called intercept term, x_1, x_2,...,x_k are the independent variables, b_i is the first-order (linear)main effect, b_{ii} is the quadratic (squared) effect, b_{ij} is the interaction effect, and ε is the random error or allows for discrepancies or uncertainties between predicted and measured values[50].The performance of the model and

significance of the statistical parameters was analyzed by ANOVA, which included the Fisher's F-test (overall model significance), Student's T-test at a probability P value of 0.05 and the determination coefficient R^2. Fig. 2 shows the general framework of using DoE in this study.

3.2. Optimization Procedure

The quadratic regression equations of Box-Behnken factorial design were used to generate the objectivefunction to estimate the optimum values of parameters. In this study, thefitness function was generated in the manner that ADS and PDI were minimized afteroptimization by the following objective function using Minitab software:

$$\text{Min}\ \ \phi(\text{ADS and PDI}),\quad \text{Constraint s}\ \ 3\langle X_1\langle 11,\quad 0\langle X_2\langle 25,\quad 10\langle X_3\langle 30$$
$$\phi = \text{ADS} \times \text{PDI} \tag{4}$$

4.Results and Discussion

4.1.ReverseMicroemulsionStability

The primary tests for determination of Span 80 wt% levels were done in pH=7 and in absence of co-surfactant. Fig. 3 shows the reverse emulsions with different Span 80wt% right after the mixing and after one hour's immobility, respectively.In the presence of the pure Span 80 (Fig.3), a milky macroemulsion was formed, which was not appropriate for nanoparticle synthesis. Similarly, in the presence of pure Tween 80, a viscous fluid similar to honey was formed instead of a reverse emulsion. After 1 hour's immobility, it could be observed that the samples with ratio higher that 40wt% of Span 80 started to sediment.

Turbiscan Lab Expert is an effective tool for monitoring the stability of emulsions and suspensions. The analyzing is based on the measurement of light transmission and backscattering of near-infrared light (NIR) source along a cylindrical vessel containing samples. The changes in transmission and backscattering are recorded versus time. According to final intensity pattern of NIR light, the destability behavior of suspension is interpreted as a function of coalescence, creaming and/or sedimentation as illustrated in Fig. 4 [51-52].

Fig. 5. Represents the transmission curves of emulsion samples containing 20, 40, and 60 wt% of span 80.

The transmission profiles of sample containing 40 wt% span 80 (Fig. 5-b) displaysa distinct clear domain (transmission100%) separated froma turbid zone (transmission 0%). The clear domain was gradually extended, which showed a mild differential sedimentation over time [53]. The droplet size of samples containing 20, 40, and 60 wt% of span 80 were measured using DLS method, which is shown in Fig. 6. The ADS of emulsions were calculated to be 447, 606 and 782 nm for 20, 40 and 60 wt% span 80 respectively. The sedimentation was higher in the sample containing 60 wt % Span 80 due to larger water droplet (ADS of 782 nm). Consequently, coalescence of droplets and differential sedimentation can be distinguished from transmission profiles (Fig. 5-c) [54].

Comparing to other concentrations, the transmission profiles for sample containing 20 wt % span 80 (Fig. 5-a) were close to the base line value for the whole height of the sample, which evidenced the good stability of emulsion at this concentration. The shape of NIR light pattern is similar to the result of Celia et al. [55] for stable vesicular drug carriers, which shows no droplet size variation during the period of analysis. Positive or negative variations of the backscattering profiles over of 18 mm height of sample containing 20 wt% span 80(Fig. 5-a) was not correlated with the destabilization processes. These variations were caused by the enclosed air on the top of the cylindrical glass tube [55, 56].

Fig.7, shows the effect of Span 80 percent (HLB) on the ADS, where the minimum range of ADS was found in the range of 10-30wt % of Span 80. Thus,a value in this domain was selected for Span 80 wt % variable in the DOE part. Fig.8 shows the reverse emulsion images right after the mixing and after 5 hour's immobility in the presence of 0.5 g different cosurfactants (at pH=7 and 40 wt % of Span80).According to Fig.8-a, the PVP had the best stabilizing effect among allused polymers. However, it appears that the polymers were not good additives for stabilizing, as shown by the quick sedimentation of reverse emulsion (Fig.8-b). Comparing to polymers, alcohol and diol had better stabilization effects, without showing any visual sedimentation (Fig.8-d).

Droplet size distributions of different alcohol and diol are shown in Fig. 9.Since the ADS of propyl alcohol (119±7.3nm) was lower than 1,2-propanediol (305±21.5 nm) and octyl alcohol (148±10.7 nm), propyl alcohol was selected as a candidate for stabilizing the RM. Moreover, the viscosity of RM was measured for different alcohols (Fig. 10). According to Fig. 10, the viscosity of RM in the presence of propyl alcohol was lower than 1,2-propanediol, which helps to a better mixing during the fission and fusion of droplets.

Therefore, the variables were selected as pH: X_1, propyl alcohol wt% in mixture of cyclohexane and propyl alcohol: X_2 and Span 80wt% in surfactant mixture: X_3 for Box-Behnken factorial design. The dependent and independent variables (with maximum, minimum and central levels) are shown in Table 1.The ASD and PDI values of reverse emulsion were chosen as the response. The PDI is a criterion of dispersity (heterogeneity of sizes of droplets) in a RM. The lower dispersity of reverse emulsion would lead to the formation of more uniform nanoparticles in droplets. Seventeen batch experiments were designed by RSM, which are given in Table 2. Table 2 also shows the experimental value (observed) of ADS and PDI for different samples based on 17 batch experimental conditions.

Fig.11 shows optical microscopy images at 20× magnification of the reverse emulsion droplets for different experimental run in Table 2.The formation, size distribution and dispersity of droplets in reverse emulsion obviously can be distinguished from Fig.11.

4.2.Coefficients of quadratic models

The determination coefficients of linear, 2-factor interaction (2FI) and quadratic models are shown in Table 3.The determination coefficient values(R^2) were found to be 0.991 and 0.975for ADS and PDI respectively, which indicating good fit of regression (Table 3). The determination coefficient is a measure of the amount of variation around the mean explained by the quadratic models.

Also the adjusted R^2 and predicted R^2values are presented in Table 3. Adjusted R^2 considered as a measure of the amount of variation around the mean explained by the model adjusted for the number of terms in the model. Predicted R^2 is a measure of the amount of variation in new data explained by the model can be applied for the evaluation of the model. The difference of adjusted R^2 values and predicted $R^2$are 0.074 and 0.041 for ADS and PDI respectively. Both values are less than 0.20 which shows there is not any problem with data or regression model[57]. The coefficients of quadratic models for ADS and PDI responses have been presented in Table 3.

Analysis of variance (ANOVA) values for the quadratic regression model are listed in Table 4. The models have an acceptable degree of accuracy if "Model F-Value" be greater than the " tabulated F-Value" at a level of significance of α.For α=0.05, degree of freedom of 9 and n=17, the tabulated F value ($F_{0.05}$, df, (n−df+1)) wasobtained equal 3.18from the standard distribution table. It can be observed that the tabular F value is clearly less than thecalculated F value of models. Therefore, the model's F value of 93.1 and 30.3 for ADS and PDI in Table 4 implies the significant of model for both responses.

In quadratic equations of ADS and PDI, the main effects of X_1, X_2, and X_3shows the average results of changing 1 variable ata time from its low-level to high level. The interaction termsX_1X_2, X_1X_3, and X_2X_3 represents how the ADS and PDI changes when two variables are simultaneously changed. With attention to the adjustment of RSM method in the present study, p-value (P) less than 0.05 shows that the relationship between the predictor and the response was statistically significant.In ADS regression model $x_1, x_3, x_1^2, x_2^2, x_3^2, x_1x_2$, x_1x_3 and x_2x_3 are significant terms while the terms of $x_1, x_2, x_3, x_1^2, x_2^2, x_3^2, x_1x_3$ and x_2x_3 are significant in PDI regression model.Both negative and positive correlation with the response may yield an unpleasant effect, depending on the system studied.

Table 5 represented the actual value (observed), predicted value and coefficient of variation (C.V.%) for eachresponse. The coefficient of variation was calculated using the following equation.

$$C.V. = \left(\sqrt{\left[\sum_{i=1}^{n} (Y_O - Y_P)^2 / (n-1)\right]} / \bar{Y}_O \times 100\right) \quad (5)$$

The coefficient of variation (C.V.) indicates thedegree of precision of conducted experiments. A relativelylower value of C.V. (5.49 and 4.84 %) indicates precision and reliabilityof the experiments [58, 59]. Similar to Meng et al., [60] the ANOVA analysis was performed to obtain the total PC values for the possible first-order, quadratic and interaction terms according to the following equations, respectively:

$$TPC_i = \frac{\sum_{i=1}^{n} SS_i}{\sum_{i=1}^{n}\sum_{j=1}^{n} SS_i + SS_{ii} + SS_{ij}} \times 100 \quad (6)$$

$$TPC_{ii} = \frac{\sum_{i=1}^{n} SS_{ii}}{\sum_{i=1}^{n}\sum_{j=1}^{n} SS_i + SS_{ii} + SS_{ij}} \times 100 \quad (7)$$

$$TPC_{ij} = \frac{\sum_{i=1}^{n}\sum_{j=1}^{n} SS_{ij}}{\sum_{i=1}^{n}\sum_{j=1}^{n} SS_i + SS_{ii} + SS_{ij}} \times 100 \quad (8)$$

where TPC_i ,TPC_{ii}, and TPC_{ij} are the total percentage contributions (TPC) of first-order, quadratic and interaction terms, respectively. Similarly, SS_i, SS_{ii}andSS_{ij} are the computed sum of squares for first-order, quadratic and interaction terms, respectively. Based on the sum of squares obtained from the ANOVA, the percentage of contributions (PC) for each individual term were estimated and illustrated in Fig.12.

Fig.12 shows that the TPC_i of first order terms and quadratic order terms had the highest level of significance with a total contribution of 57 and 74 % as comparing to other TPC values in the ADS and PDI, respectively.

4.4.Optimization studies for reverse microemulsion conditions

The output functions of RSM method were used as an objective function Eq.(4) for theoptimization process using Minitab software.

Table 6shows the results of optimum process parameters and thoseobtained from the RMs that were synthesized in lab. Fig. 13-a shows the trend of fitness function value during the minimization and optimum values. Fig. 13-b shows the affect of each factor on the responses. The vertical red lines on the graph represent the current factor settings. The numbers displayed at the top of a column show the current factor level settings (in red). The horizontal blue lines and numbers represent the responses for the current factor level. Minitab calculates that ADS and PDI are minimized when all factors are at X_1=5.98, X_2 (wt.%)=8.08 and X_3 (wt.%)=26.56.

The Fig.14 shows the stability test anddroplet size distribution (3measurements with 1 min interval) of RM at optimum condition just after production.

According to Fig.14-a stable transparent microemulsion with 42 nmaverage droplet size was obtained under the optimum conditions. The ADS of RM by passing time (Fig. 14-c) shows no significant change for ADS for long time of several months, which confirm formation of RM.

The results of this study confirmed the increasing stability of reverse emulsions by using a mixture of surfactants. The optimum value of 12.15 for HLB in this studywas close to the optimum value of 10 in Noor El-Din et al.[26] formixed sorbitan monooleate and polyoxyethylene sorbitan monooleate surfactants in water-in-diesel fuel nanoemulsions. The HLB value was far away fromsuggested optimization range of 3-6 from Williams [25]. This is because of using Span 80 and Tween 80 surfactant’s mixturewould producesynergic effects on the properties of emulsion.There was an optimum ratio wherethe best balance between the arrangements of surfactant molecules in the interfacial region of water droplets was reached. The Span 80 molecules are oil soluble and would consolidate by spreading in oil phase. On the other hand Tween 80 molecules are water soluble and the formation of hydrogen bonds between hydroxyl group and water molecules would consolidate in water phase. At the optimum balance, the strength of interfacial film reaches to the best situation, preventing from the deformation of droplets by external force, and hence a lowed polydispersity.

Increasing the amount of cosurfactant changes the relative oil and water solubility of surfactants. So there is an optimum value for cosurfactant to achieve the best solubility of surfactants [61].In this study all of the cosurfactants studied improved the RM stability but the alcohols achieved the best results. This observation is consistence with Azeem et al. [33]who examined the affect of ethanol, isopropyl alcohol, n-butanol, PEG 400, Carbitol, and propylene glycol as cosurfactants. As alcohol molecules have a weak amphiphile behavior in water/oil mixture,they participate in the interfacial region of droplets and form dense surfactant molecules, leading to the reduction of the water uptake and the droplet size [32].In fact, in the presence of alcohol, the interfacial tension between oil and water droplets decreased, producing smaller droplets. However under high alcohol concentration, the increasing attractive inter droplet interaction could produce a reversed effect and so an optimum amount of alcohol is desired to form microemulsions[62]. The optimum value of 8 was obtained for propyl alcohol wt% in mixture of cyclohexane and propyl alcohol.

When surfactant molecules adsorbs on the interface of droplets, the interfacial tension between the two phases would decrease before the CMC. Adsorbed surfactants stabilize emulsions via either steric stabilization or electrostatic stabilization. Water droplets in continuous oil emulsioncan be considered as conducting particles in a non-conducting media. In fact, the ions are trapped and spread interior in the water droplet and cause the formation of a thin double layer around droplets, which cannot exhibit any electrostatic repulsion. In general, electrostatic stabilization is significant only for oil in water emulsions since the electric double layer thickness is much greater in water than in oil. According to Table 1 and Fig. 11, in the acidic and alkali media, the polydispersity of droplets has increased. This is probably because of the destructive effect of OH^- and H^+ ions on the formation of alcohol-surfactant hydrophilic head complex which need further study.

Fig. 15 shows the 3D response surfaces as the functions of two variables at the optimum level of other variables.

The optimum conditions of RM according to Table 6 (pH=5.98, HLB=12.15, propyl alcohol wt% in mixture of cyclohexane =8.08) were used to synthesis iron oxide nanoparticles. Fig. 15 illustrates the procedure of iron oxide nanofluid production. After completion of reaction, the nanoparticles are dispersed inside RM environment (Fig. 15-a), Organic phase separation from

aqueous phase was performed by destabilization of RM through addition and mixing of 4 ml de-ionized water to final suspension reaction (Fig. 15-b).The final iron oxide nanoparticles were transfer from organic phase to water phase by phase transformation technique. The phase transformation approach is based on movement of nanoparticles between organic-aqueous phases through modification of particle's surface ligands. The work of Sperling and Parak [63] showed that such modification could transfer the formed nanoparticles from the original nonpolar environment (i. e., organic phase) to a polar aqueous phase. By adding one droplets of acid citric and mixing, iron oxide nanoparticles were transferred from the organic phase to the water phase(Fig. 16-c). The addition of acid produces a new layer of surfactant molecules on the original ligand of nanoparticle surface which has been discussed and confirmed in advance in our previous study [12].Final Iron oxide nanofluid was produced by separation of water phase containing nanoparticles form organic phase and addition of 30 ml extra ionized water (Fig. 16-d) [12].

Fig. 17-a,b shows HRTEM photos of iron oxide nanoparticles which were synthesized under the optimum RM conditions (pH=5.98, HLB=12.15, propyl alcohol wt% in mixture of cyclohexane =8.08). Fig. 17-c shows the size distribution of nanoparticles which was estimated using image processing by photoshop 7 software. Pretty uniform spherical nanoparticle distribution with 2.1±0.49 nanometer average size and polydispersity of 0.06±0.011 was obtained by the RM method. The comparison of ultra small monodisperse iron oxide nanoparticles with a precise size control of 1 nm in this study with other methods in the literature such as thermal decomposition (4-20 nm) [64], sol-gel (9-12 nm) [65], sonochemical (30-40 nm) [66] and electro-oxidation (20-30 nm) [66] shows the excellent capability of proposed approach. EDEX analysis of iron oxide nanoparticles showed a strong peak in graph at 6.4 keV (Fig. 17-d) corresponding to the iron element. An extra peak of carbon and cupper were observed on EDEX graph, which was due to the carbon coated copper TEM grids used.

5. Conclusion

Optimized formation of RM, particularly for nanoparticle synthesis was studied by the Box-Behnken factorial design. The pH, co-surfactant amount and HLB were selected in the design of

experiments method as the important factors that influence the average size and polydispersity index of the reverse emulsion droplets. The determination coefficients of 0.991 and 0.975 for average size and polydispersity index respectively showed the good fit of quadratic regression. The values of pH=5.98, propyl alcohol/mixture of cyclohexane and propyl alcohol=8.08wt% and span80/surfactant mixture=26.56wt% were obtained as the optimum parameters through the optimization process. At the optimum conditions, a RM with average droplet size equal 42±3.2nanometer and polydispersity index equal 0.41±0.041was achieved. Also the uniform iron oxide nanoparticles with average particle size of 2.1±0.49and polydispersity of 0.06±0.011was produced by using RM at optimum conditions.

References

[1] H. Wennerstrom, J. Balogh and U. Olsson, Interfacial tensions in microemulsions, Colloids and Surfaces A: Physicochemical and Engineering Aspects, 291(2006) 69-77.

[2] J. H. Schulman and J. B. Montagne, Formation of microemulsions by amino alkyl alcohols, Annals of the New York Academy of Sciences, 1961, 92, 366-371.

[3] D. J. McClements, Nanoemulsions versus microemulsions: terminology, differences, and similarities, Soft Matter, 8 (2012) 1719-1729.

[4] M. A. Malik, M. Y. Wani, M. A. Hashim, Review: Microemulsion method: A novel route to synthesize organic and inorganic nanomaterials, 5 (2012) 397-417.

[5] Achinta Bera, Ajay Mandal, Microemulsions: a novel approach to enhanced oil recovery: a review,Journal of Petroleum Exploration and Production Technology, 5 (2015) 255-268.

[6]N. Garti, Microemulsions as microreactors for food applications, Current Opinion in Colloid and Interface Science, 8 (2003) 197-211.

[7]P. Boonme , Applications of microemulsions in cosmetics, J. Cosmet. Dermatol, 6 (2007) 223-228.

[8]W. Zhang, X. Qiao, J. Chen, Review Synthesis of silver nanoparticles-Effects of concerned parameters in water/oil microemulsion, Materials Science and Engineering B, 142 (2007) 1-15.

[9] R.A. Martinez-Rodriguez, F.J. Vidal-Iglesias, J. Solla-Gullon, C. R. Cabrera, and J. M. Feliu, Synthesis of Pt Nanoparticles in Water-in-Oil Microemulsion: Effect of HCl on Their Surface Structure, J. Am. Chem. Soc. 136 (2014) 1280-1283.

[10]K.Pemartin, C. Solans , J. Alvarez-Quintana, M. Sanchez-Dominguez, Synthesis of Mn-Zn ferrite nanoparticles by the oil-in-water microemulsion reaction method, Colloids and Surfaces A: Physicochemical and Engineering Aspects, 451 (2014) 161-171.

[11] C.Okoli, M.Sanchez-Dominguez, M.Boutonnet, S. Jaras, C. Civera, Conxita Solans, G.. Rajarao Kuttuva, Comparison and Functionalization Study of Microemulsion-Prepared Magnetic Iron Oxide Nanoparticles, Langmuir, 28 (2012) 8479-8485.

[12]E. Nourafkan, M. Asachi, H. Gao, G. Raza, D. Wen, Synthesis of stable iron oxide nanoparticle dispersions in high ionic media, Journal of Industrial and Engineering Chemistry, 50 (2017) 57-71.

[13] E. Nourafkan and A. Alamdari, Study of effective parameters in silver nanoparticle synthesis through method of reverse microemulsion, Journal of Industrial and Engineering Chemistry, 20 (2014) 3639-3645.

[14] A. Hu, Z. Yao, X. Yu, Phase behavior of a sodium dodecanol allyl sulfosuccinic diester/n-pentanol/methyl acrylate/butyl acrylate/water microemulsion system and preparation of acrylate latexes by microemulsion polymerization, J. Appl. Polym. Sci. 113 (2009) 2202-2208.

[15] M.P. Pileni, Nanocrystals: fabrication, organization andcollective properties, C.R. Chimie. 6 (2003) 965-978.

[16] S. May, A. Ben-Shaul, Molecular Theory of the Sphere-to-Rod Transition and the Second CMC in Aqueous Micellar Solutions, J. Phys. Chem. B. 105 (2001) 630-640.

[17] C. Petit, P. Lixon, M.P. Pileni, In situ synthesis of silver nanocluster in AOT reverse micelles, J. Phys. Chem. 97 (1993) 12974-12983.

[18] M.A. Lopez-Quintela, C. Tojo, M.C. Blanco, L. Garcia Rio, J.R. Leis, Microemulsion dynamics and reactions in microemulsions,Current Opinion in Colloid & Interface Science,9 (2004) 264-278.

[19] C.Y. Tai, C. Chen, Particle morphology, habit, and size control of $CaCO_3$ using reverse microemulsion Technique, Chemical Engineering Science, 63 (2008) 3632-3642.

[20] W. Zhang, X. Qiao, J. Chen, Synthesis and characterization of silver nanoparticles in AOT microemulsion system, Chemical Physics, 330 (2006) 495-500.

[21] C.M. Pey, A. Maestro, I. Sole, C. Gonzalez, C. Solans, J.M. Gutierrez, Optimization of nano-emulsions prepared by low-energy emulsification methods at constant temperature using a factorial design study, Colloids and Surfaces A: Physicochem. Eng. Aspects. 288 (2006) 144-150.

[22] S.Shahriar, Effect of mixing protocol on formation of fine emulsions, Chem. Eng. Sci. 61 (2006) 3009-3017.

[23] L.Dai, W. Li, X. Hou, Effect of the molecular structure of mixed nonionic surfactants on the temperature of miniemulsion formation,Colloids and Surfaces A: Physicochemical and Engineering Aspects, 125(1997) 27-32.

[24] H. Sagitani, S.E. Friberg, Microemulsion systems with anonionic cosurfactant. J. Dispers. Sci. Technol. 1(1980) 151-164.

[25] D.F. Williams, Chemistry & Technology of the cosmetics and toiletries industries, Cosmetics & Toiletries, Springer, 2003.

[26] M.R. Noor El-Din, S.H. El-Hamouly, H.M. Mohamed, M.R. Mishrif, A.M. Ragab,Water-in-diesel fuel nanoemulsions: Preparation, stabilityand physical properties, Egyptian Journal of Petroleum, 22 (2013) 517-530.

[27] A. Bumajdad, J. Eastoe, Conductivity of mixed surfactant waterinoil microemulsions, Physical Chemistry Chemical Physics,6(2004) 1597-1602.

[28] Y., Barakat, L.N. Fortney, R.S. Schechter, W.H. Wade, S. Yiv, A. Graciaa, Criteria for structuring surfactants to maximize solubilizationof oil and water: II. Alkyl benzene sodium sulfonates, Colloid. Interface. Sci. 92(1983) 561-574.

[29] K.R. Wormuth, E.W. Kaler, Amines as microemulsion cosurfactants, J. Phys. Chem. 91 (1987) 611-617.

[30] L.J. Maidment, V. Chen, G.G. Warr, Effect of added cosurfactanton ternary microemulsion structure and dynamics, Colloids. Surf. A. 129(1997) 311-319.

[31] F.I. Abd-Allah H.M.Dawaba, A.M.Ahmed,Development of a microemulsion-based formulation to improve the availability of poorly water-soluble drug, Drug Discoveries and Therapeutics,4 (2010) 257-66.

[32] D.S. Mathew R.S. Juang,Review: Role of alcohols in the formation of inverse microemulsionsand back extraction of proteins/enzymes in areverse micellar system, Separation and Purification Technology, 53 (2007) 199215.

[33] A.Azeem, M.Rizwan, F. J. Ahmad, Z. Iqbal, R. K. Khar, M. Aqil, S. Talegaonkar, Nanoemulsion Components Screening and Selection: a Technical Note, AAPS. Pharm. Sci. Tech. 10 (2009) 69-76.

[34]L.Yang , R. Xie , L. Liu , D. Xiao , J. Zhu, Synthesis and Characterization of ZnSe Nanocrystals by W/O Reverse Microemulsion Method: The Effect of Cosurfactant, J. Phys. Chem. C. 115 (2011) 19507-19512.

[35] Q. Chen,X. Shen , H. Gao , Formation of nanoparticles in water-in-oil microemulsions controlled by the yield of hydrated electron: the controlled reduction of Cu2+,J. Colloid. Interface. Sci. 308(2007)491-499.

[36] J.D. McLean, P.K. Kilpatrick, Effects of asphaltene aggregationin model heptane – toluene mixtures on stability of water-in-oilemulsions, Journal of Colloid and Interface Science, 196 (1997) 23-34.

[37] J.G. Sjoblom, L. Mingyuan, A.A. Christy, T. Gu, Water-in-crude oil emulsions from theNorwegian continental shelf interfacial pressure and emulsion stability, Colloid and Interface Science, 66 (1992) 55-62.

[38] S.M. Hashmi, A. Firoozabadi, Self –assembly of resins and asphaltenes facilitates asphaltene dissolutionby an organic acid. Journal of Colloid and Interface Science, 394 (2013) 115-123.

[39] M.A. Usman, E.T. Evwierhoma and I.I. Onuoha, Asphaltene Solvency and Stability of Water in Oil Emulsion: ACase Study of Two Nigerian Crudes, Journal of Energy Technologies and Policy, 3 (2013) 16-29.

[40] J.E. Strassner, Effect of pH on Interfacial Films and Stability of Crude Oil-Water Emulsions, J. Pet. Technol. 20 (1968) 303-312.

[41] M.Daaou, D. Bendedouch, Water pH and surfactant addition effects on the stability of an Algerian crude oil emulsion, Journal of Saudi Chemical Society, 16 (2012) 333-337.

[42] Z. Jeirani, B. M. Jan, B. S. Ali, I. M. Noor ,S. C. Hwa, W. Saphanuchart,The optimal mixture design of experiments: Alternative method in optimizing theaqueous phase composition of a microemulsion, Chemometrics and Intelligent Laboratory Systems, 112 (2012) 1-7.

[43] S. Sood, K. Jain , K. Gowthamarajan , Optimization of curcumin nanoemulsion for intranasal delivery using design of experiment and its toxicity assessment, Colloids. Surf. B. Biointerfaces. 113 (2014) 330-337.

[44] V. Polychniatou C. Tzia, Study ofFormulation and Stability of Co-surfactant Free Water-in-Olive Oil Nano- and Submicron Emulsions with Food Grade Non-ionic Surfactants, Am. Oil. Chem. Soc. 91 (2014) 79-88.

[45] M.A. Malik, M.Y. Wani, M. A. Hashim, Microemulsion method: A novel route to synthesize organicand inorganic nanomaterials, Arabian JournalofChemistry,5 (2012) 397-417.

[46] R. Massart, Preparation of aqueous magnetic liquids in alkaline and acidic media, IEEE Trans Magn. 17 (1981) 1247-1248.

[47] R.M. Myers, D.C. Montgomery, Response surface methodology, 2nd ed., New York: Wiley, 2002.

[48] R.K. Deshmukh, J.B. Naik, Aceclofenac microspheres: quality by design approach. Mater. Sci. Eng. C., 36 (2014) 320-328.

[49] D.C.Montgomery, Design and analysis of experiments. JohnWiley & Sons, 1991.

[50] A. Bjorck, Numerical Methods for Least Squares Problems, SIAM, Society for Industrial and Applied Mathematics, 1996.

[51] H. Buron, O. Mengual, G. Meunier, I. Cayre, P. Snabre,ReviewOptical characterization of concentrateddispersions: applications to laboratoryanalyses and on-line process monitoringand control, Polymer International, 53(2004)1205-1209.

[52] O. Mengual, G. Meunier, I. Cayre, K. Puech, P. Snabre, TURBISCAN MA 2000: multiple light scatteringmeasurement for concentrated emulsion and suspensioninstability analysis, Talanta 50 (1999) 445-456.

[53] C. Chauvierre, D. Labarre, P. Couvreur, C. Vauthier,A new approach for the characterizationof insoluble amphiphilic copolymers basedon their emulsifying properties, Colloid Polym. Sci. 282 (2004) 1097-1104.

[54]K. Muthurania, Z. Jin, J. Williams, S. Ohtake, Investigation of the Sedimentation Behavior of Aluminum Phosphate: Influence of pH, Ionic Strength, and Model Antigens, Journal of Pharmaceutical Sciences, 104 (2015) 3770-3781.

[55] C. Celia, E. Trapasso, D. Cosco, D. Paolino, M. Fresta,Turbiscan Lab® Expert analysis of the stability of ethosomes® andultradeformable liposomes containing a bilayer fluidizing agent, Colloids and Surfaces B: Biointerfaces, 72 (2009) 155-160.

[56] W. Kang, B. Xu, Y. Wang, Y. Li, X. Shan, F. An, J. Liu, Stability mechanism of W/O crude oil emulsion stabilized by polymer andsurfactant, Colloids and Surfaces A: Physicochem. Eng. Aspects, 384 (2011) 555-560.

[57] T.F. Coleman, Y. Li, On the Convergence of Reflective Newton Methods for Large-Scale Nonlinear Minimization Subject to Bounds, Math. Prog., 67 (1994) 189-224.

[58] Y. Zhang, J. Zhang, Optimization of headspace solid-phase microextraction for analysis of ethyl carbamate in alcoholic beverages using a face-centered cube central composite design, Analytica chimica acta, 627 (2008) 212-218.

[59] M. Ghasemnejad, E. Ahmadi, Z. Mohamadnia, A. Doustgani , S. Hashemikia, Functionalized silica nanoparticles as a carrier for Betamethasone Sodium Phosphate: Drug release study and statistical optimization of drug loading by response surface method, Materials Science and Engineering C, 56 (2015) 223-232.

[60] H., Meng, X. Hu and A. Neville, A systematic erosion-corrosion study of two stainlesssteels in marine conditions via experimental design, Wear, 263 (2007) 355-362.

[61] Z. Jeirani, B. Mohamed Jan, B. Si Ali, I.M. Noor, C.H. See, W. Saphanuchart, Formulation, optimization and application of triglyceride microemulsionin enhanced oil recovery, Industrial Crops and Products 43 (2013) 6-14.

[62] R. Kohli, K.L. Mittal, Developments in Surface Contamination and Cleaning, William Andrew, ISBN : 9781437778793, 2013.

[63] R.A. Sperling, W.J. Parak, Review: Surface modification, functionalizationand bioconjugation of colloidalinorganic nanoparticles, Phil. Trans. R. Soc. A. 368 (2010) 1333-1383.

[64] P. Guardia, A.Labarta, X. Batlle, Tuning the size, theshape, and the magnetic properties of iron oxide nanoparticles, J. Phys. Chem. C., 115 (2010) 390-396.

[65] H. Qi, B. Yan, W. Lu, C. Li, Y. Yang, A non-alkoxidesol-gel method for the preparation of magnetite (Fe_3O_4)nanoparticles, Curr. Nanosci., 7 (2011) 381-388.

[66] L. Cabrera, S. Gutierrez, N. Menendez, M.P. Morales, P. Herrasti, Magnetite nanoparticles: electrochemicalsynthesis and characterization, Electrochim. Acta., 53 (2008) 3436-3441.

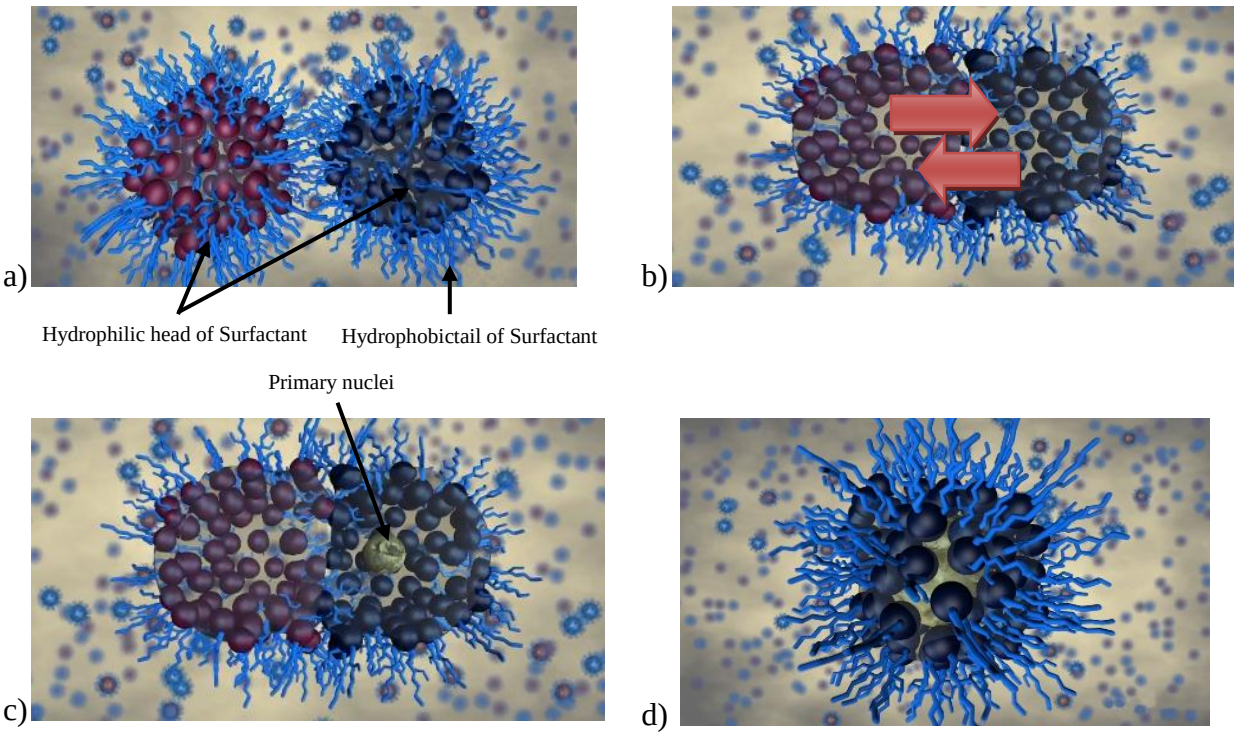

Fig. 1. Mechanism of formation of nanoparticles in a RM, a) collision of nanodroplets containing different precursors, b) exchange of precursors during fusion and fission, c) formation primary nuclei and growth mechanism, and d) stabilization of nanoparticle.

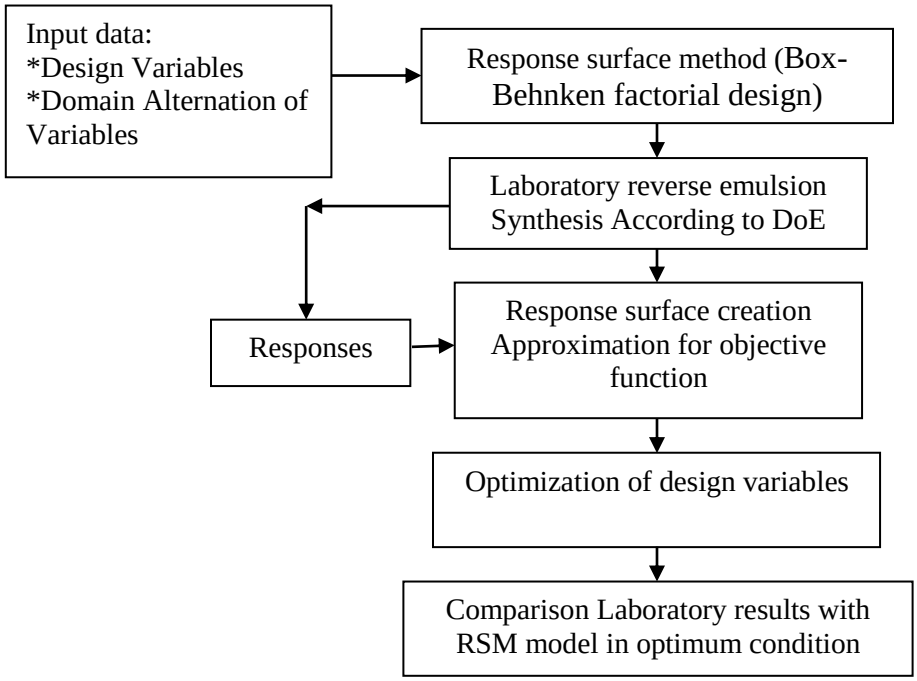

Fig.2.The general framework of RSM design and optimization process.

a)

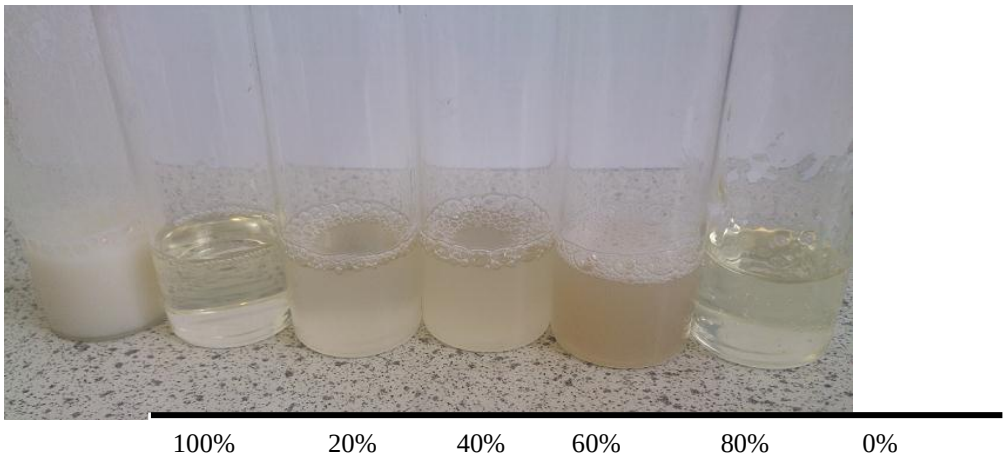

Fig. 3. The reverse emulsions were synthesized using different wt% of Span 80 (pH=7 and in absence of any co-surfactant) just after mixing.

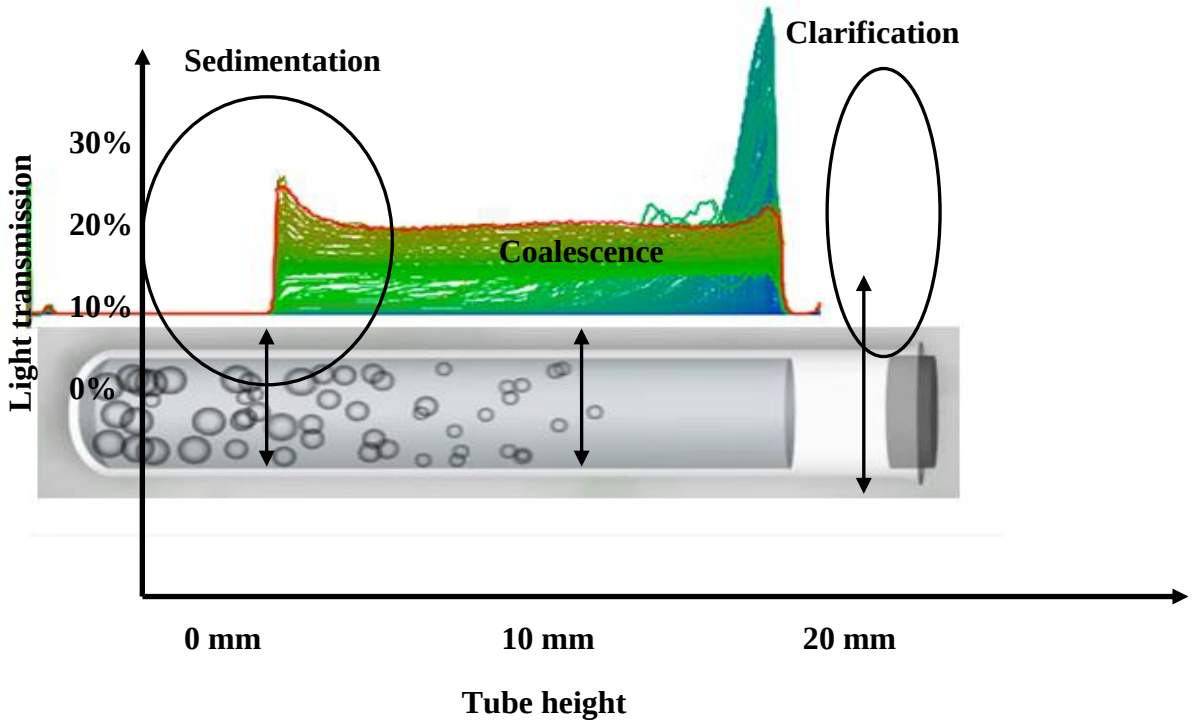

Fig. 4. Example of detection coalescence and sedimentation using Turbiscan transmission profile.

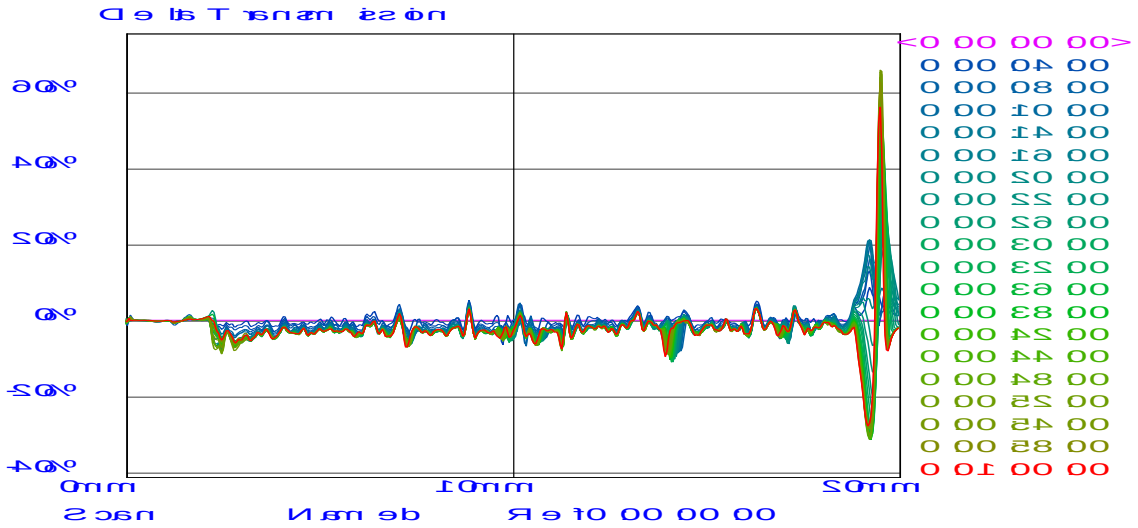

a)

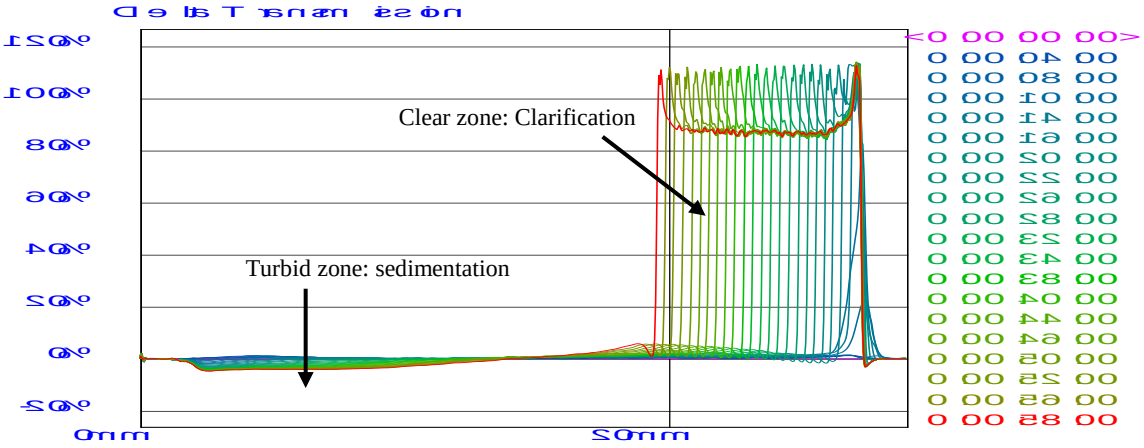

b)

c)

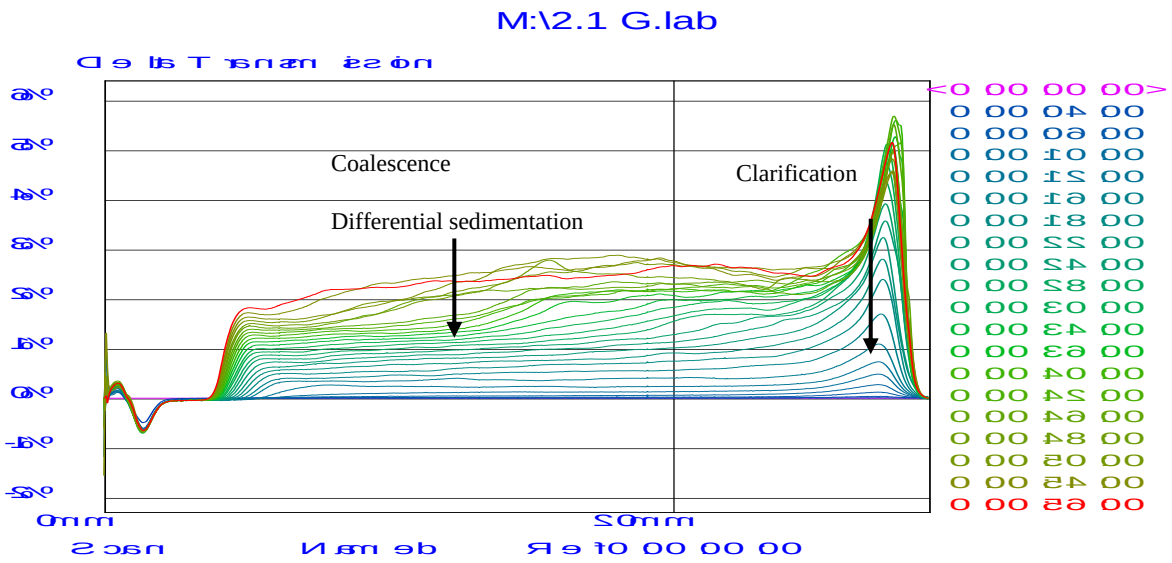

Fig.5.Transmissionprofilesof reverse emulsion containing a) 20,b)40 and c) 60wt % Span80using Turbiscan Lab Expert (pH=7 and in absence of any co-surfactant) just after samples preparation.

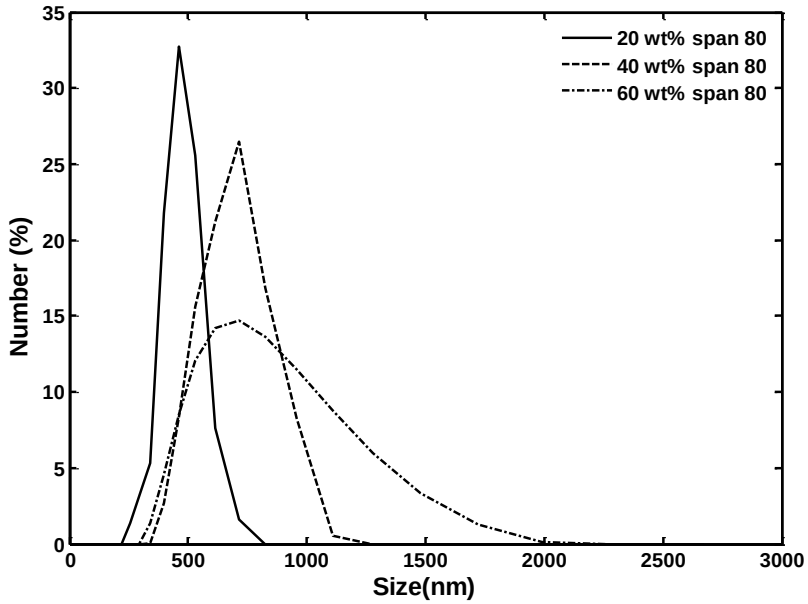

Fig. 6. Droplet size distribution of reverse emulsion at different weight percent of span 80 surfactant.

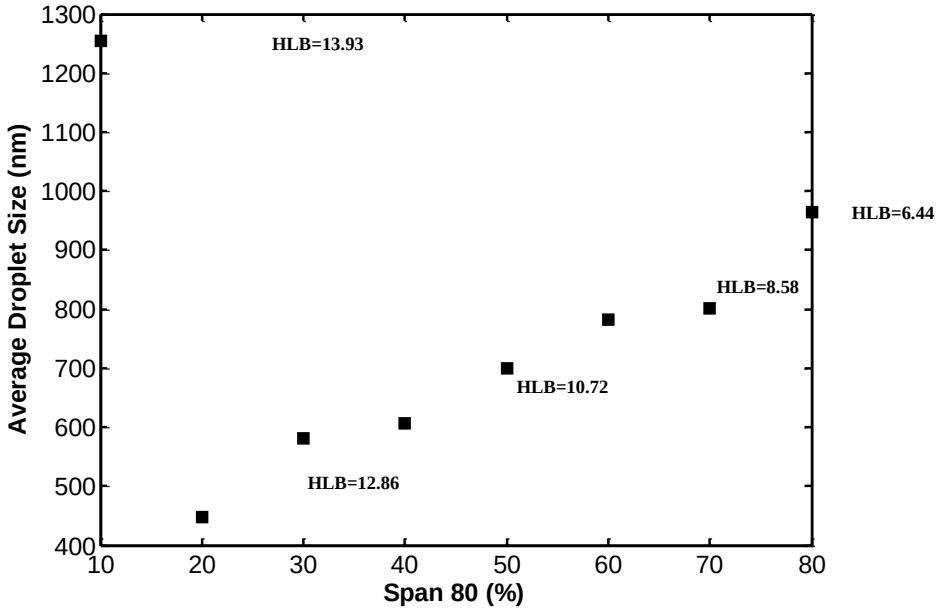

Fig.7.Effect of Span 80 wt % (HLB) on average droplet size distribution.

a) b)

c) d)

Fig. 8. The reverse emulsions were synthesized with adding 0.5 g of different (at pH=7 and 40 wt% of Span80), a,b) polymer cosurfactant mixing, c,d) alcohol and diol cosurfactant.

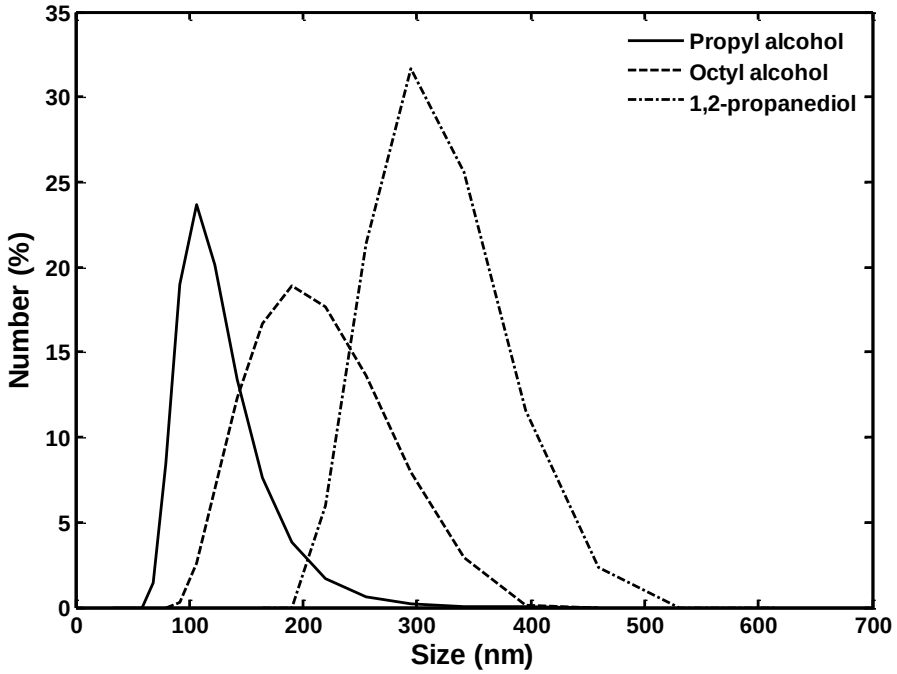

Fig. 9. Droplet size distribution of reverse emulsion for alcohol and diol cosurfactant.

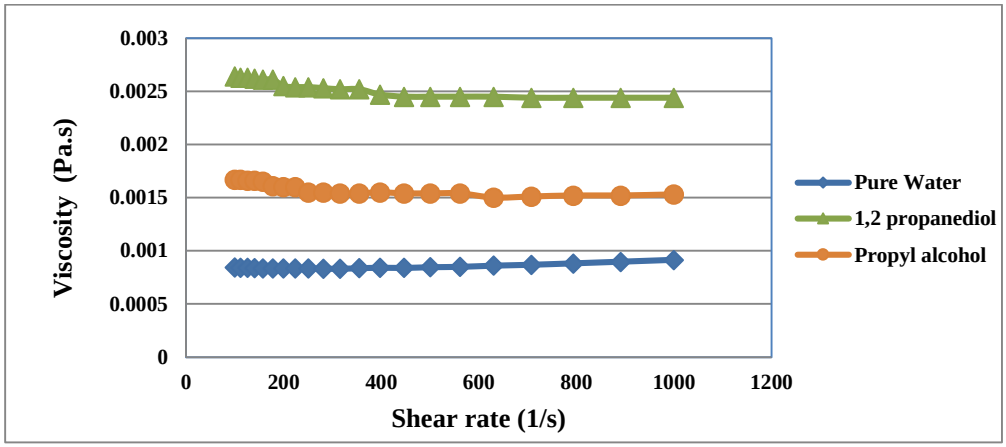

Fig. 10. The viscosity versus shear rate for RMs containing different alcohols.

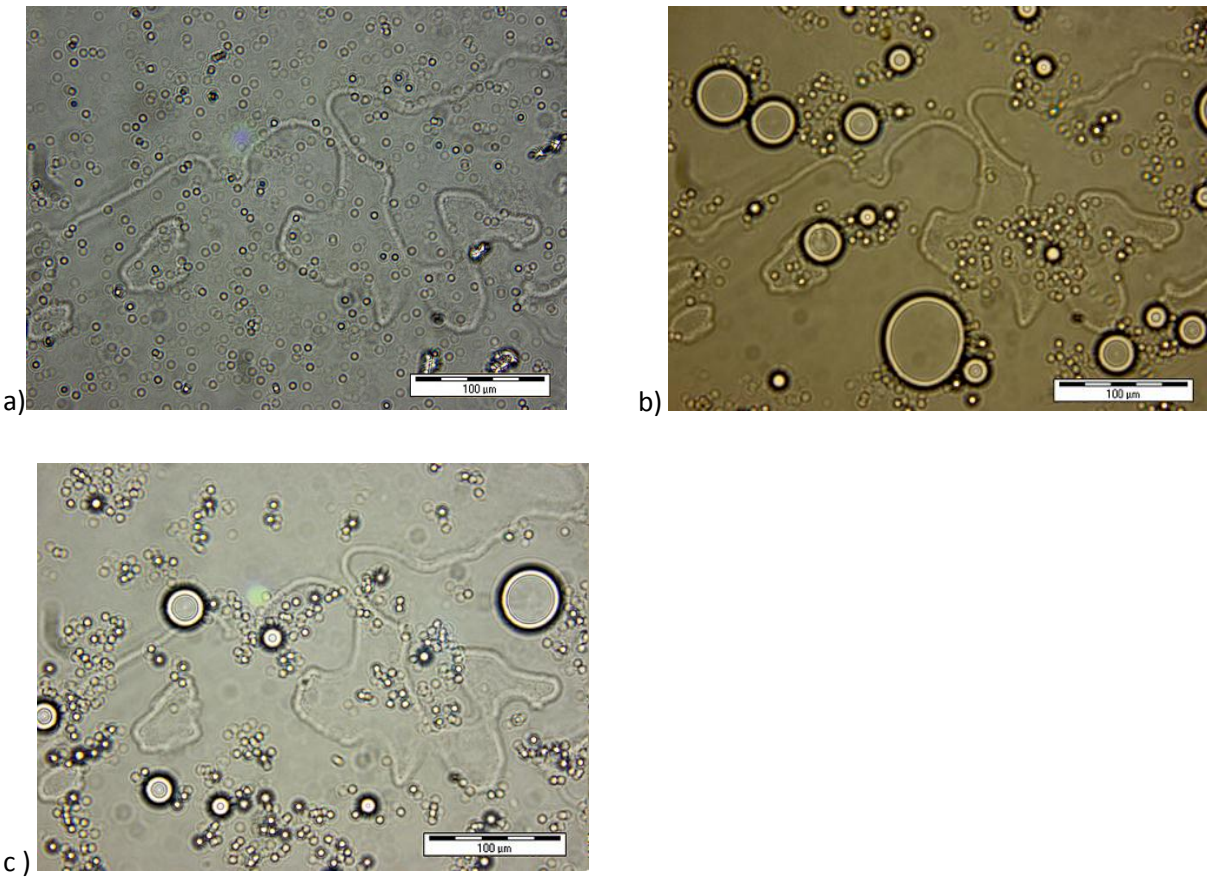

Fig.11. Optical microscopy image at 20× magnification for different experimental run a) no. 6, b) no. 9 and c) no. 17.

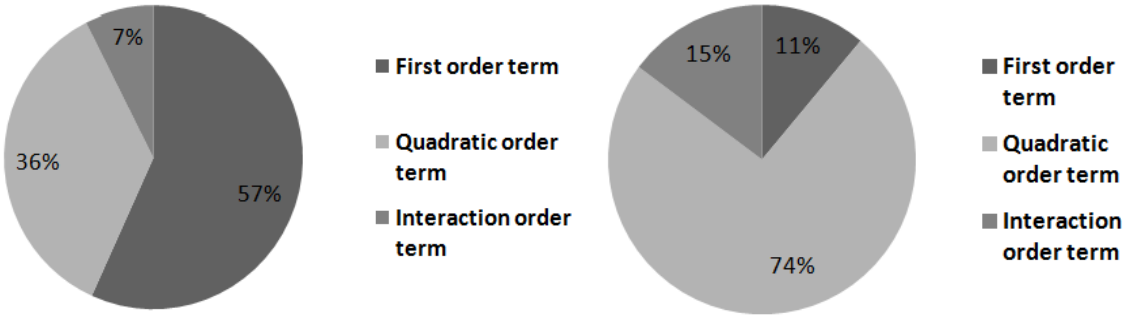

a) b)

Fig.12.A detailed schematic showing the percentage contributions of components for a) ADS and b) PDI.

a)

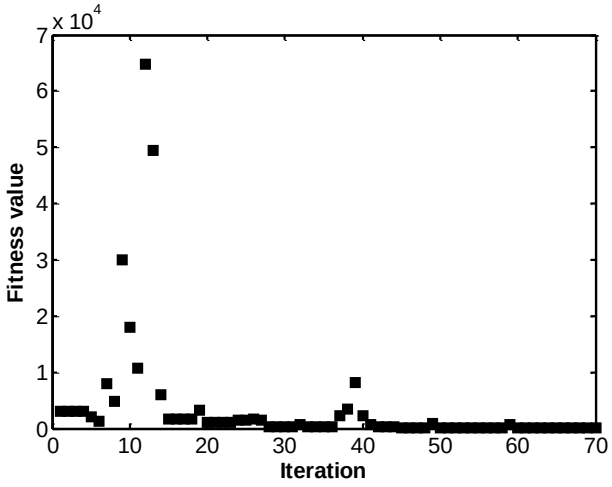

b)

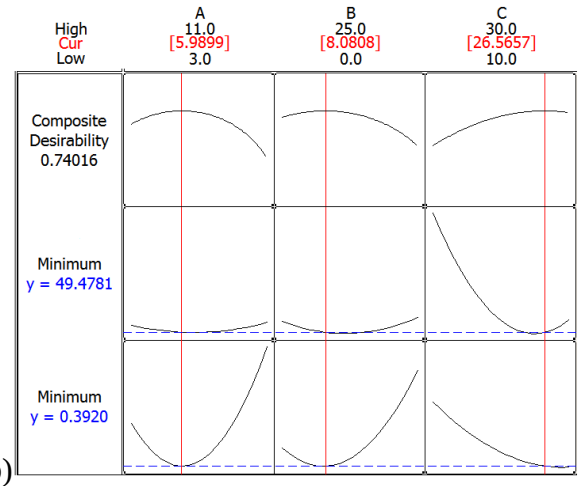

Fig. 13. a) The trend of fitness function value b) affect of each factor on the responses.

a)

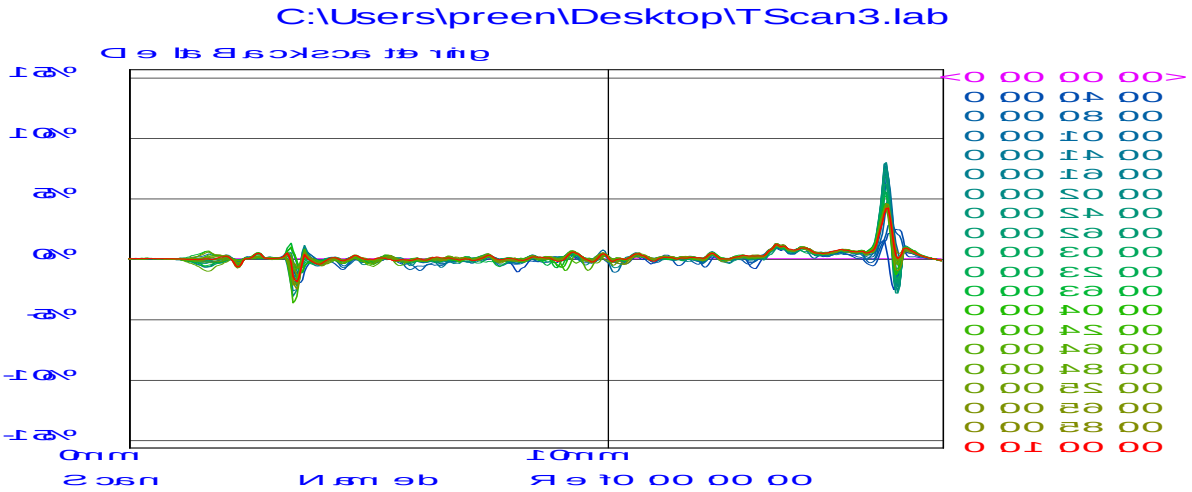

b)

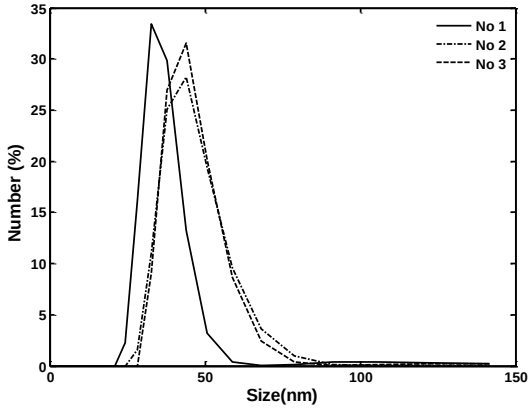

c)

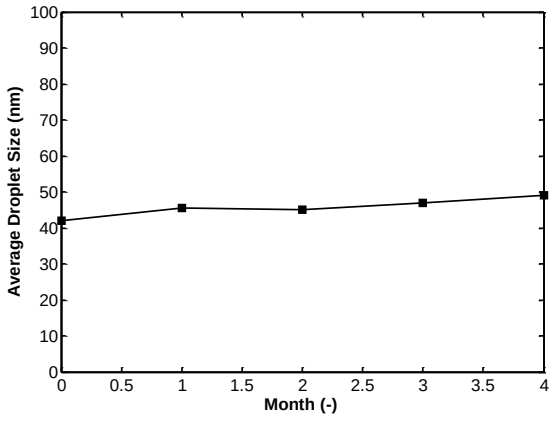

Fig.14. a) The stability test, b) droplet size distribution of RM at optimum condition, c) ADS of RM versus time.

a)

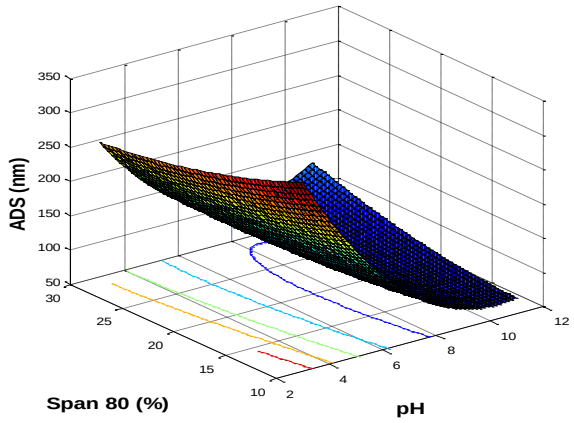

b)

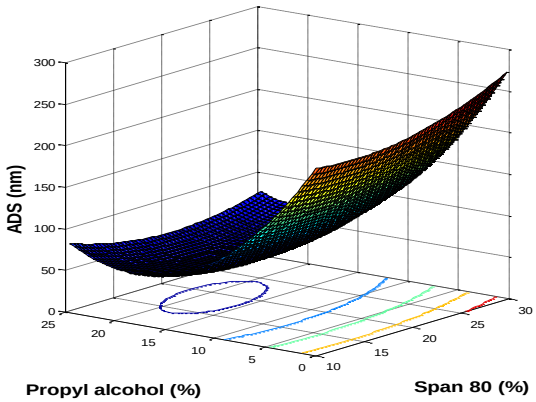

c)

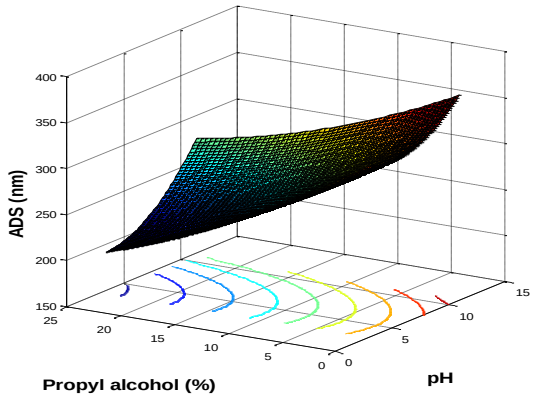

d)

e)

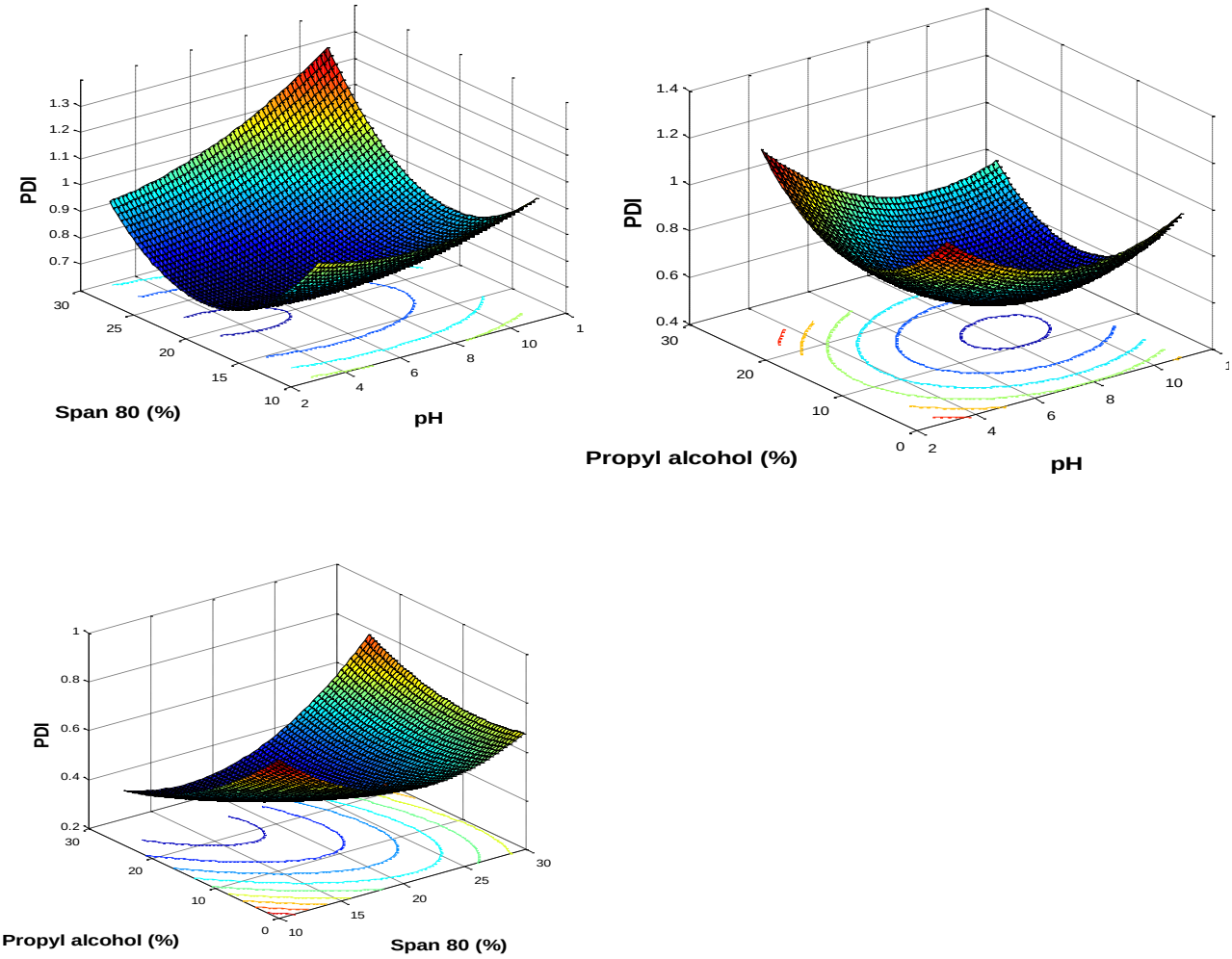

f)

Fig. 15. The combined effect of a)pH and span 80, b) span 80 and propyl alcohol, c) pH and propyl alcohol on ADS; The combined effect of d)pH and span 80, e) span 80 and propyl alcohol, f) pH and propyl alcohol on ADS

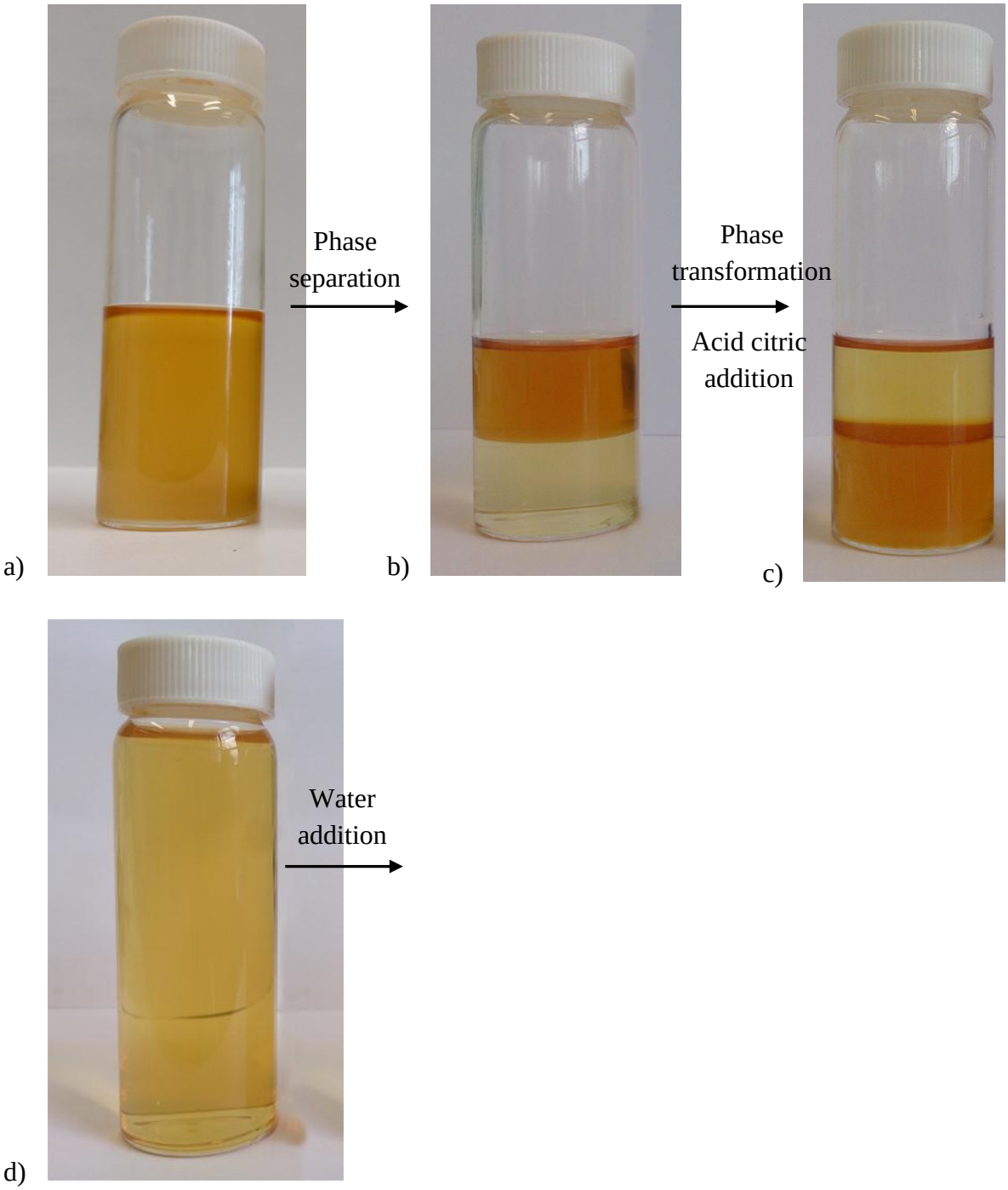

Fig. 16. a) the suspension reaction just after reaction, b) phase separation of reaction suspension after addition de-ionized water, c) phase transformation by adding one droplet acetic acid, d) nanofluid of iron oxide after mixing with extra de-ionized water.

a) 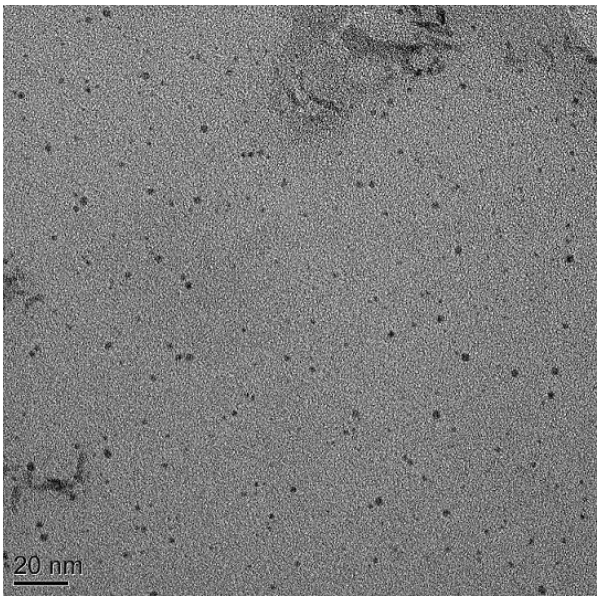

b) 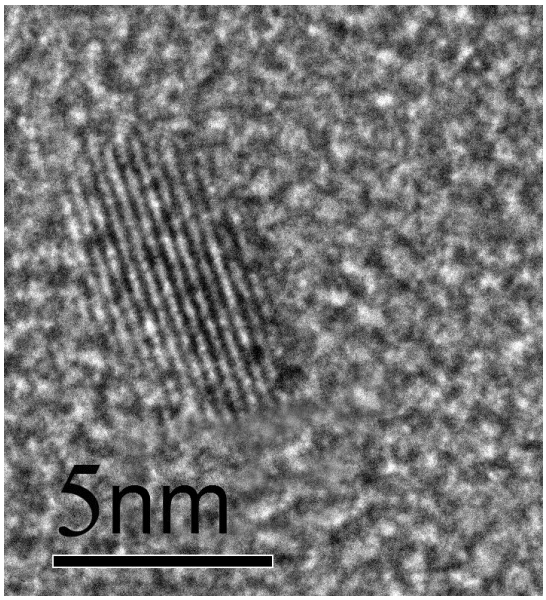

a) 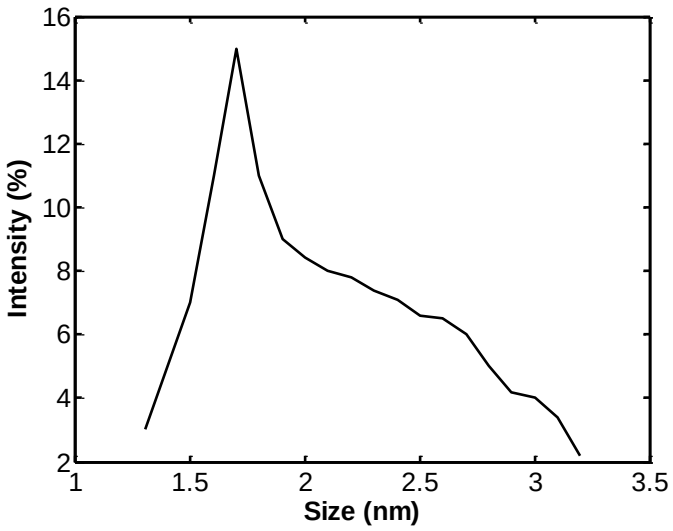

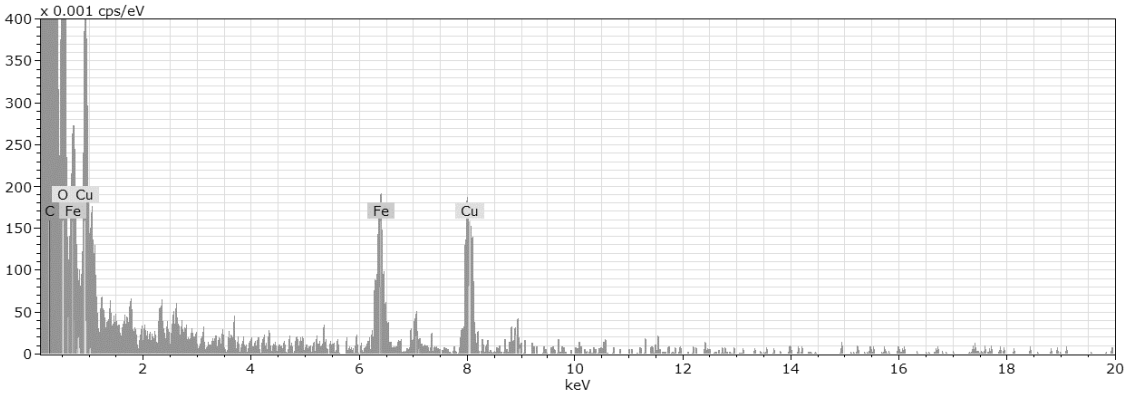

d)

Fig. 17. a, b) HRTEM photo, c) size distribution and d) EDEX analysis of iron oxide nanoparticle with 2 nanometer average size which has been synthesized in optimum RM.

Table 1. The dependent and independent variables.

Independent variable	Low level (-1)	Medium level (0)	High level (+1)
X_1: pH	3	7	11
X_2: propyl alcohol in mixture of cyclohexane and propyl alcohol (wt%)	0	12.5	25
X_3: Span 80 in surfactant mixture (wt%)	10	20	30
Dependent variables			
Y_1 = Average droplet size, ADS, (nm)			
Y_2 = Polydispersity index, PDI,			

Table 2. Box-Behnken design matrix with three independent variables and observed output responses

No	Level of parameters				Output responses (Observed)	
	X_1	X_2	X_3		ADS (nm)	PDI
1	3	12.5	30		57±4.3	0.61±0.065
2	3	0.0	20		105±13.6	0.74±0.056
3	7	25.0	30		91±6.8	0.81±0.023
4	7	12.5	20		68±2.4	0.48±0.031
5	11	25.0	20		112±19.3	1±0.00
6	7	12.5	20		71±5.6	0.34±0.033
7	7	0.0	10		207±17.1	0.85±0.048
8	11	12.5	30		93±14.3	0.91±0.084
9	3	12.5	10		288±16.2	0.85±0.042
10	7	12.5	20		62±4.8	0.43±0.036
11	11	0.0	20		48±9.5	1.0±0.00
12	7	12.5	20		51±2.8	0.44±0.020
13	3	25.0	20		120±13.9	0.92±0.012
14	7	25.0	10		255±22.1	0.68±0.078
15	7	12.5	20		65±3.1	0.51±0.048
16	7	0.0	30		98±3.2	0.43±0.017
17	11	12.5	10		183±16.9	0.81±0.071

Table 3.Summary of regression analysis for responses.

Models	**R^2**	**Adjusted R^2**	**Predicted R^2**
ADS (nm)			
Linear	0.56	0.46	0.24
2-factor interaction	0.63	0.42	0.00
Quadratic	0.991	0.981	0.907
PDI			
Linear	0.11	0.00	0.00
2-factor interaction	0.27	0.00	0.00
Quadratic	0.975	0.902	0.943
Suggested regression equations of the fitted models			
$Y_1 = 719.2 - 35.96 X_1 - 1.54 X_2 - 43.88 X_3 + 0.79 X_1^2 + 0.13 X_2^2 + 0.79 X_3^2 + 0.24 X_1 X_2 + 0.88 X_1 X_3 - 0.11 X_2 X_3$			
$Y_2 = 2.21 - 0.266 X_1 - 0.041 X_2 - 0.061 X_3 + 0.018 X_1^2 + 0.00119 X_2^2 + 0.00067 X_3^2 - 0.00087 X_1 X_2 + 0.0021 X_1 X_3 + 0.001 X_2 X_3$			

Table 4.Some statistical value formodel parameters whichwere obtained fromANOVA table.

Factor	**DF**	**ADS**			**PDI**		
		Sum of squares	**F**	**p value**	**Sum of squares**	**F**	**p value**
Model	9	84774	93.1	0.000	0.75	30.36	0.000
X_1	1	2244	47.7	0.000	0.043	95.8	0.000
X_2	1	1800	1.3	0.293	0.017	34.8	0.001
X_3	1	44104	385.6	0.000	0.023	27.38	0.001
X_1^2	1	1402	6.6	0.036	0.38	126.69	0.000
X_2^2	1	2501	16.9	0.004	0.15	53.0	0.000
X_3^2	1	26394	261	0.000	0.019	6.9	0.034
X_1X_2	1	600	5.94	0.045	0.007	2.77	0.140
X_1X_3	1	4970	49.1	0.000	0.029	10.83	0.013
X_2X_3	1	756	7.4	0.029	0.074	26.8	0.001
Residual Error	7	707			0.019		
Lack of fit	3	470	2.64	0.185	0.003	0.26	0.854
Pure Error	4	237			0.016		

Table 5. The observed results and predicted valuesfor responses

No	ADS (nm)			PDI		
	Y_{pre}	Y_{obs}	% Error	Y_{pre}	Y_{obs}	% Error
1	61.04	57	6.61	0.578	0.61	5.53
2	109.63	105	4.22	0.749	0.74	1.20
3	87.84	91	3.59	0.817	0.81	0.856
4	62.35	68	9.06	0.438	0.48	9.58
5	104.98	112	6.68	0.987	1	1.31
6	62.35	71	13.87	0.438	0.34	22.37
7	207.99	207	0.47	0.837	0.85	1.55
8	97.04	93	4.16	0.897	0.91	1.44
9	281.34	288	2.36	0.861	0.85	1.27
10	62.35	62	0.56	0.438	0.55	1.82
11	51.23	48	6.30	0.983	1.000	1.72
12	62.35	51	18.20	0.438	0.44	0.45
13	115.3	120	4.07	0.928	0.92	0.86
14	265.24	255	3.86	0.656	0.68	3.65
15	62.35	65	4.25	0.438	0.51	16.43
16	85.59	98	14.49	0.453	0.43	5.07
17	176.5	183	3.68	0.835	0.81	2.99

Mean of predict	116.11	0.692
Mean of observe	115.02	0.794
SS_E	735.03	0.020
C.V.%	5.49	4.84

Table 6. The results of optimum process parameters and experiments.

Optimum parameters			**Output response**		
X_1	X_2 (wt.%)	X_3 (wt.%)		ADS	PDI
5.98	8.08	26.56 (HLB=12.15)	Predicted	49.47	0.39
			Experimental	42±3.2	0.41±0.041
			Error %	15%	4.8%